

بسم الله الرحمن الرحيم

000000

تم رقع هذه الرسالة بواسطة / سلوي محمود عقل

بقسم التوثيق الإلكتروني بمركز الشبكات وتكثولوجيا المطومات دون أدنى مسنولية عن محتوى هذه الرسالة.

NA		T R	ملاحظات:
4 1	6997		
	AIMSWAM	R. CIVILLE HARINA	
1	5/15/20	1992	- 1 3 m. f

بمكات وتكنولوجبارته



Role of Ultrasonography and Color Doppler Imaging in Identification of Thyroid Nodules Suspicious of Malignancy for Fine Needle Aspiration

Thesis

Submitted for Partial Fulfilment of Master Degree in Radiology

Presented by

Ahmed Mohamed Hussein Kamel

M.BB.Ch. - Ain Shams University

Supervised by

Assist. Prof. Dr Zenat Ahmed El-Sabbagh

Assistant Professor of Radiodiagnosis Faculty of Medicine - Ain Shams University

Dr. Ali Hagag Ali

Lecturer of Radiodiagnosis
Faculty of Medicine - Ain Shams University

Faculty of Medicine Ain Shams University 2021



سورة البقرة الآية: ٣٢

Acknowledgment

First and foremost, I feel always indebted to **ALLAH**, the Most Kind and Most Merciful.

I'd like to express my respectful thanks and profound gratitude to Assist. Prof. Dr. Zenat Ahmed El-Sabbagh, Assistant Professor of Radiodiagnosis, Faculty of Medicine - Ain Shams University for her keen guidance, kind supervision, valuable advice and continuous encouragement, which made possible the completion of this work.

I am also delighted to express my deepest gratitude and thanks to **Dr. Ali Hagag Ali,** Lecturer of Radiodiagnosis, Faculty of Medicine - Ain Shams University, for his kind care, continuous supervision, valuable instructions, constant help and great assistance throughout this work.

Ahmed Mohamed Hussein

List of Contents

Title	Page No.
List of Abbreviations	i
List of Tables	ii
List of Figures	iii
Introduction	1
Aim of the Work	3
Review of Literature	
Anatomy of the Thyroid Gland	4
Sonographic Anatomy of the Thyroid Gland	10
Pathology of Thyroid Nodules	13
Ultrasound Features of Thyroid Nodules	28
Role of Doppler US in Risk Stratification	47
Patients and Methods	52
Results	58
Illustrative Cases	74
Discussion	84
Summary and Conclusion	89
References	
Arabic Summary	

List of Abbreviations

Abb.	Full term
ACR	. American College of Radiology
Ant. Strap m	. Anterior strap muscle
ATA	. American Thyroid Association
CCA	. Common carotid artery
CFD	. Color flow Doppler
ETE	. Extrathyroidal extension
FMTC	Familial medullary thyroid carcinomas
FNA	. Fine Needle Aspiration
FTC	. Follicular Thyroid carcinoma
HCC	. Hürthle or oncocytic cell cancer
IJV	. Internal jugular vein
IQR	. Inter-quartile range
MEN	Multiple endocrine neoplasia
MTC	. Medullary thyroid carcinoma
NPV	. Negative predictive value
PD	. Power Doppler
PDTC	. Poorly differentiated thyroid carcinoma
PI	. Pulsatility index
PPV	. Positive predictive value
PRF	. Pulse repetition frequency
PSV	. Peak Systolic Velocity
PTC	. Papillary thyroid carcinoma
RI	. Resistive index
ROC	. Receiver operating characteristic curve
SCM	. Sternocleidomastoid muscle
SPSS	. Statistical Package for Social Science
TIRADS	. Thyroid Imaging, Reporting, and Data System
TSH	. Thyroid-stimulating hormone
	. Ultrasonography
	World Health Organization

List of Tables

Table No.	Title	Page No.
Table (1):	Etiology of thyroid nodules	13
Table (2):	Papillary Thyroid Carcinoma Variants	
Table (3):	Sonographic characteristics summarizes their published m sensitivities and specificities for det of malignancy	nedian ection
Table (4):	Comparison between benign group malignant group of the studied cases.	
Table (5):	Comparison between benign group malignant group regarding age and the studied cases, and site of the node	sex of
Table (6):	Comparison between benign group malignant group regarding maximum dimension and TIRADS score	n axial
Table (7):	Comparison between benign group malignant group regarding PSV and the intranodular vessels	RI of
Table (8):	The diagnostic performance of the TI and doppler	

List of Figures

Fig. No.	Title	Page No.
Figure (1):	The thyroid gland Anatomy of the thyroid gland	
Figure (2): Figure (3):	Transverse section of the neck at (showing relationships of the thyroid	C6 level
Figure (4):	Blood supply and venous drainage thyroid gland	
Figure (5):	The lymphatic drainage of the gland is extensive and flows multidirectional pattern	in a
Figure (6):	Transverse US image of the n thyroid isthmus level	
Figure (7):	Normal sonographic appearance of gland and its relations	•
Figure (8):	Transverse image of a pyramid (arrow) in a patient with surgical a of the left lobe	absence
Figure (9):	The thyroid lobe contains an encap follicular adenoma	
Figure (10):	Hyalinizing trabecular tumor nuclear grooves and nuclear	with pseudo
	inclusions	
Figure (11):	Papillary thyroid carcinoma	
Figure (12):	Papillary thyroid carcinoma	
Figure (13):	Minimally invasive follicular car showing a thick fibrous capsule	
	focus of transcapsular invasion	
Figure (14):	Lymph nodes of importance in	
118410 (11)	carcinoma	-
Figure (15):	C-cell hyperplasia (Hematoxylin &	Eosin) 25
Figure (16):	Anaplastic carcinoma	27

List of Figures Cont...

Fig. No.	Title	Page No.
Figure (17):	ACR TI-RADS scoring system flow	
Figure (18):	A well differentiated papillary	
g	cancer in the left thyroid	•
Figure (19):	Markedly hypoechoic nodule	
Figure (20):	Internal content	34
Figure (21):	Cystic papillary cancer	35
Figure (22):	The soft tissue component	36
Figure (23):	Four partially cystic isoechoic	nodules
	showing typical spongiform appeara	ance 37
Figure (24):	Microcalcifications within thyroid n	odule 38
Figure (25):	Entirely cystic nodule shows n comet-tail artifacts	-
Figure (26):	An enlarged heterogeneous thyroic with biopsy proven microcalcifications	benign
Figure (27):	A 4-mm papillary thyroid carcinoma mid-right thyroid	
Figure (28):	Central linear macrocalcifications with posterior acoustic shadowing	(arrow)
Figure (29):	A smooth peripheral rim of "eg calcification	ggshell"
Figure (30):	Hypoechoic solid nodule with a lol margin	bulated
Figure (31):	Thick, irregular, and incomplet surrounding solid iso- to hype	e halo erechoic
E! (90)		43
Figure (32):	Isoechoic nodule with thin regular l	
Figure (33):	This anaplastic carcinoma shows extrathyroidal extension anteriorly	

List of Figures Cont...

Fig. No.	Title	Page No.
Figure (34):	Metastatic lymph nodes	46
Figure (35):	Peripheral vascularity in a spon nodule	_
Figure (36):	Peripheral and intranodular vasc in a hypoechoic nodule	-
Figure (37):	Ultrasonographic examination of year-old male patient	a 40-
Figure (38):	A female patient with follicular card	
Figure (39):	Pie chart demonstrating percent male and female patients	age of
Figure (40):	Pie chart demonstrating the site nodules	of the
Figure (41):	Pie chart demonstrating the Tascore among the patients	IRADS
Figure (42):	Pie chart demonstrating the Tascore among the patients	IRADS
Figure (43):	Pie chart demonstrating the FNA re	
Figure (44):	Chart demonstrating comparison be benign group and malignant regarding age of the studied cases	etween group
Figure (45):	Chart demonstrating the sex of malignant and benign groups	of the
Figure (46):	Chart demonstrating comparison be benign group and malignant regarding site of the nodules	etween group
Figure (47):	Chart demonstrating comparison be benign group and malignant regarding size of the nodules	group
Figure (48):	Chart demonstrating comparison be benign group and malignant regarding TIRADS score	etween group

List of Figures Cont...

Fig. No.	Title	Page	No.
Figure (49):	Chart demonstrating FNA results f		68
Figure (50):	Chart demonstrating comparison benign group and malignant regarding PSV of the intranodular	group	70
Figure (51):	Chart demonstrating comparison benign group and malignant regarding RI of the intranodular ve	group	71
Figure (52):	Graph demonstrating the specificity TIRADS	y of the	
Figure (53):	Graph demonstrating the specificity intranodular vessels RI	-	72
Figure (54):	Case 1		74
Figure (55):	Case 2		75
Figure (56):	Case 3		76
Figure (57):	Case 4		76
Figure (58):	Case 5		77
Figure (59):	Case 6		79
Figure (60):	Case 7		79
Figure (61):	Case 8		81
Figure (62):	Case 9		82
Figure (63):	Case 10	•••••	83



Introduction

Ultrasonography (US) is one of the most widely used imaging technologies in medicine. It is portable, free of radiation risk, and relatively inexpensive when compared with other imaging modalities, such as magnetic resonance and computed tomography the images can be acquired in "real time," thus providing instantaneous visual guidance for many procedures including those for regional interventional anesthesia and pain management (Chan & Perlas, 2011).

Thyroid nodules are exceedingly common, with a reported prevalence of up to 68% in adults on high-resolution US (Tessler et al., 2017).

Certain features of thyroid nodules on US consistently predictive of malignancy and are used as criteria for Fine Needle Aspiration (FNA). These criteria have various sensitivity and specificity, but unfortunately none of them alone is sufficient to discard or detect malignancy efficiently (Russ et al., 2017).

FNA of the thyroid is the single most useful diagnostic test for evaluating the patients with thyroid nodules who should undergo surgery (Renshaw et al., 2020).

Medical professional societies such as the American Thyroid Association (ATA) and American Association of Clinical Endocrinologists have suggested that the initial



cytological diagnosis can be postponed until growth of a nodule or a change in its US features is observed. Repeated FNA of nodules with an initial benign cytological diagnosis leads to a final diagnosis of cancer in approximately 2% of cases (Maino et al., 2021).

The pattern of vascularity and intra-nodular peak systolic velocity can be used as color and spectral Doppler parameters differentiate benign from malignant thyroid nodules. Intranodular flow is strongest predictor for diagnosing malignancy among color Doppler parameters (Bhatt et al., *2017*).

Since about 90% of thyroid nodules are benign, it is crucial to correctly stratify the malignancy risk of the nodules to avoid a huge number of unnecessary invasive procedures and/or surgery, as an improper use of FNA has the risk of increasing healthcare expenditures and even of inappropriately referring patients to surgery in case of indeterminate cytology (*Pantano et al.*, 2018).

AIM OF THE WORK

The aim of the study is to investigate the performance of US imaging and color flow mapping in identification of thyroid nodules indicated for FNA to predict thyroid cancer to avoid unnecessary interventions.

Chapter 1

ANATOMY OF THE THYROID GLAND

Thyroid gland is the largest endocrine gland. It is situated opposite C5- C7 and T1 vertebra embracing anterolateral part of trachea. The gland is related medially to trachea and esophagus and carotid sheath laterally. The gland is covered anterolaterally by sternocleidomastoid and three ribbon muscles, sternohyoid, sternothyroid and superior belly of omohyoid muscles (*Singh*, 2020).

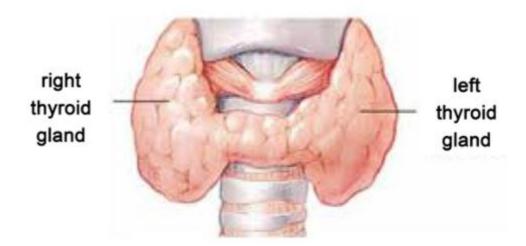


Figure (1): The thyroid gland (Quoted from Arrangoiz et al., 2018).

The shape of the thyroid gland varies from an H to a U shape and is formed by two lateral lobes with superior and inferior poles connected by a median isthmus (**Figure 1**), with an average height of 12 to 15 mm, overlying the second to fourth tracheal rings. Each of the lateral thyroid lobes measures an average of 50 to 60 mm (8 to 10 ml in volume), with the